Journal of Photonics for Energy

SPIEDigitalLibrary.org/jpe

Cu(In,Ga)Se_2 thin-film solar cells based on a simple sputtered alloy precursor and a low-cost selenization step

Veronika Haug
Ines Klugius
Theresa Magorian Friedlmeier
Aina Quintilla
Erik Ahlswede

SPIE

$Cu(In,Ga)Se_2$ thin-film solar cells based on a simple sputtered alloy precursor and a low-cost selenization step

Veronika Haug, Ines Klugius, Theresa Magorian Friedlmeier, Aina Quintilla, and Erik Ahlswede
Zentrum für Sonnenenergie- und Wasserstoff-Forschung Baden-Württemberg (ZSW), Industriestraße 6, D-70565 Stuttgart, Germany
ines.klugius@zsw-bw.de

Abstract. High-efficiency thin-film solar cells based on $Cu(In,Ga)Se_2$ are often formed by depositing precursor films and using a subsequent selenization step. We demonstrate a simple and cost-efficient approach simplifying both process steps by using a ternary Cu-In-Ga alloy target for sputter deposition of the precursor layer and by using a simple nonvacuum selenization reaction based on elemental selenium. In this contribution we examine in detail the characteristics of the precursor layers. The sputter growth is governed by a segregation of In-rich islands on top of a closed Cu-rich base. With optimized layers we could achieve conversion efficiencies well above 13% without the use of antireflective coating or metallic grids. The influence of the selenization duration on morphology and performance is discussed. [DOI: 10.1117/1.3659500]

Keywords: photovoltaics; solar cells; $Cu(In,Ga)Se_2$; thin film; sputtering; selenization; ternary target.

Paper 11190R received Jun. 15, 2011; revised manuscript received Aug. 25, 2011; accepted for publication Oct. 20, 2011; published online Nov. 8, 2011.

1 Introduction

$Cu(In,Ga)Se_2$ (CIGS)-based solar cells have the highest potential of all thin-film solar cells with record efficiencies exceeding 20%.[1] CIGS layers are conventionally deposited in high-vacuum chambers using either thermal co-evaporation of the elements, including selenium,[2] or sequential sputtering of Cu, In, and Ga with subsequent selenization.[3,4] Using sequential sputtering, the highest efficiencies of more than 16% could be demonstrated by Johanna Solar for a rather complex and costly pentanary system $Cu(In,Ga)(Se,S)_2$ from sputtered bilayer structures of CuGa and In, treated first in H_2Se and subsequently in H_2S.[5] A similar process was originally developed by Siemens and improved by Showa Shell and is called the sulfurization after selenization method.[6]

Although these processes are very promising, a further reduction of process complexity and production costs is desirable. Up to now, most sputter-based fabrication methods work with more than one target and thus require the control of several cathodes which makes the process quite complex. A single-target approach avoids this challenge. Recent publications deal with the development of such a Cu-In-Ga (CIG) alloy target,[7,8] whereas first results could be demonstrated using alloy targets leading to cell efficiencies exceeding 6%.[9,10] We demonstrate a simple fabrication method for CIGS solar cells employing such an alloy target. The cell efficiencies well over 13% indicate a high potential for cost reduction. The selenization is made with a nonvacuum setup to avoid expensive vacuum equipment and sophisticated selenization reactors. Furthermore, it employs elemental selenium instead of highly toxic H_2Se.

1947-7988/2011/$25.00 © 2011 SPIE

2 Experimental Details

CIG precursor layers are sputter-deposited on Mo-covered glass substrates from one single target without any grading within the layer. The target is made from microalloyed powder from Heraeus with 48.5 at.% copper, 38.5 at.% indium, and 13 at.% gallium.[8] Standard parameters of 0.5 W/cm^2 dc power, an Ar flow of 30 sccm, and no additional heating of the substrate were applied. Deposition time and process gas pressure was varied from 100 to 2000 s and 1 to 15 μbar, respectively.

The samples were selenized in a simple tubular furnace in nitrogen-diluted selenium vapor slightly below atmospheric pressure (for safety reasons), similar to the setups described in Refs. 11 and 12. A continuous flux of nitrogen carries the selenium vapor along the sample reaction zone. The intrinsic temperature gradient within the furnace is used to establish a sample temperature of about 550°C while the crucible with the elemental selenium is placed at the edge region of the furnace at about 400°C to 500°C. The process time was varied between 2 and 90 min.

Absorber layers are completed using conventional methods by a CdS buffer layer, a ZnO window layer, and a ZnO:Al layer to obtain a complete solar cell, as described in Ref. 13.

The film morphology of precursor layers as well as of selenized layers was studied with a scanning electron microscope (SEM) (XL30 SFEG Sirion from FEI Company); energy-dispersive x-ray spectroscopy (EDX) measurements were carried out with a Noran detector in the same instrument. The precursor surface was measured by a three-dimensional (3D) laser scanning microscope VK9700 from Keyence. Secondary neutral mass spectrometry (SNMS) measurements were made with a SSM 200 from Leybold. The crystallinity is monitored by x-ray diffraction (XRD), performed with a Siemens D5000 (copper target) at 40 kV and 40 mA tube voltage and current, respectively. X-ray fluorescence analysis (XRF) is performed at 10^{-1} mbar in an EAGLE XXL system, equipped with an energy-dispersive Si (Li) detector and a 50 kV Rh x-ray source. Current-voltage curves were measured using a Keithley 238 source-measure unit under simulated AM 1.5 global solar irradiation with a ORIEL sun simulator at 100 mW/cm^2 to extract the basic solar cell characteristics from devices of approximately 0.24 cm^2 in size.

3 Results and Discussion

3.1 Precursor Characterization

SEM cross-sections and 3D microscope measurements of precursor layer surfaces are shown in Fig. 1. We observe a phase-segregated morphology consisting of a closed, compact underlayer and a rough, irregular top layer. For increasing deposition time, the closed underlayer increases linearly, while it decreases for increasing sputter gas pressure. As expected, the overall film thickness increases linearly with sputter time and decreases slightly with sputter pressure (determined via XRF, data not shown).

Purwins et al.[14] described the existence of a two-phase regime in the Cu-In-Ga phase diagram, consisting of elemental indium together with the copper-rich $Cu_{16}(In_{1-y},Ga_y)_9$ and/or $Cu_9(In,Ga)_4$ phases. Indeed, our XRD measurements of a precursor indicate the existence of elemental indium as well as $Cu_{16}(In_{1-y},Ga_y)_9$ and/or $Cu_9(In,Ga)_4$ within the layer (see Fig. 2). It was not possible to distinguish between the two phases within the XRD pattern. Furthermore, it is not clear if this phase combination evolves during the sputtering or if it is already present in the target.

The atomic composition determined by EDX of the underlayer and the top layer is shown in Table 1. The atomic ratio CGI = Cu/(Ga+In) of ca. 1.8 for the underlayer fits well to the copper-rich $Cu_{16}(In_{1-y},Ga_y)_9$ phase. The top layer contains much more In than the underlayer and we hence expect In to be present as a mixed alloy along with the Cu-In-Ga phase(s).

The sputtered film generally contains less copper and less gallium than the original target. The graph in Fig. 3 shows the average atomic concentration of precursors which were sputtered

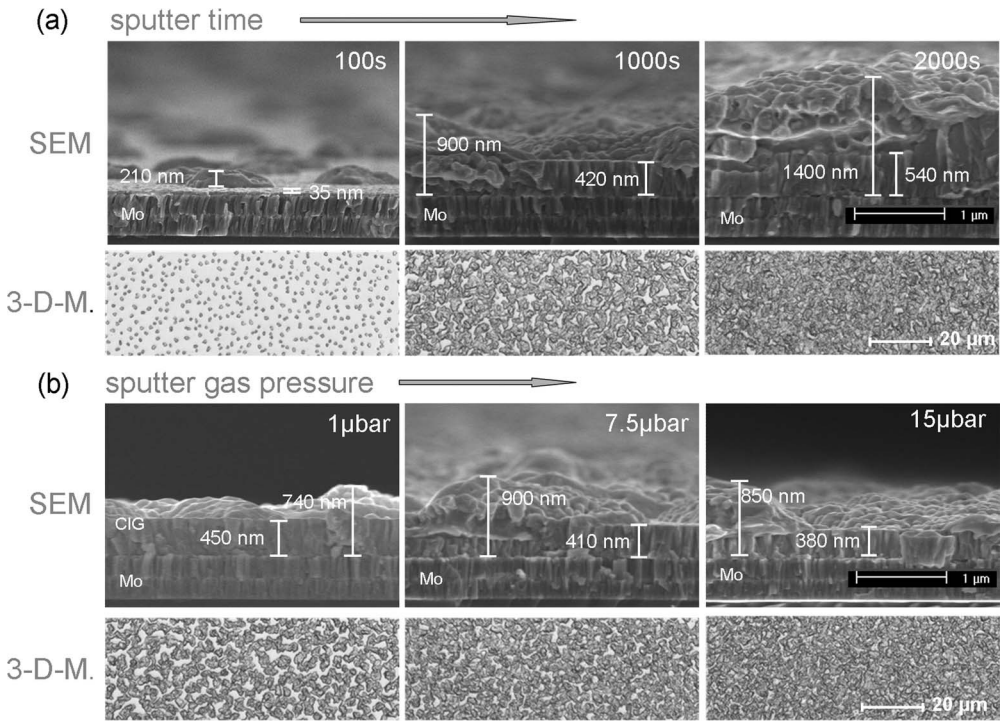

Fig. 1 SEM cross sectional images and 3D microscope measurements of the layer surfaces of (a) precursors sputtered at 100, 1000, and 2000 s and at a constant gas pressure of 2.5 μbar and (b) precursors sputtered at 1, 2.5, and 15 μbar and at a constant sputter time of 1000 s.

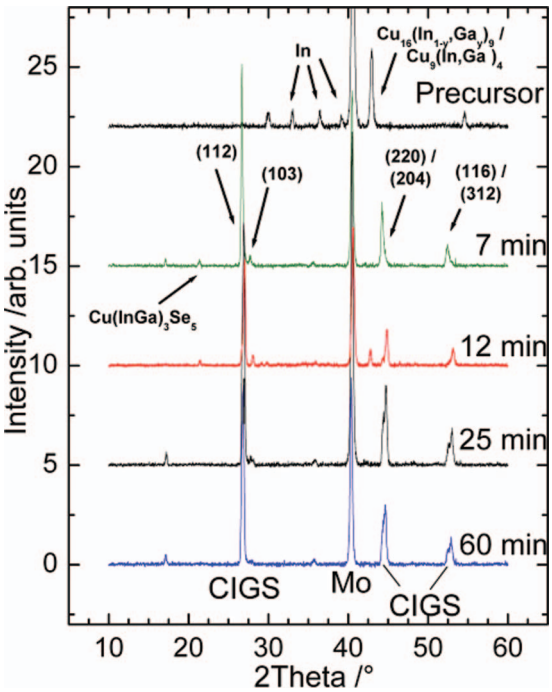

Fig. 2 XRD data for a precursor layer and selenized layers of various selenization durations. The diffractogram of the precursor indicates the existence of elemental indium as well as $Cu_{16}(In_{1-y},Ga_y)_9$ and/or $Cu_9(In,Ga)_4$ within the layer. For selenized layers, all undesired crystalline phases have vanished after 25 min and only CIGS can be found.

Table 1 The atomic composition of the underlayer and the top layer of a sputtered precursor, determined by EDX measurement, as well as the resulting atomic ratio CGI = Cu/(Ga+In).

EDX	Cu / at.%	In / at.%	Ga / at.%	CGI
Top layer	44	48	8	0.79
Underlayer	64	21	15	1.78

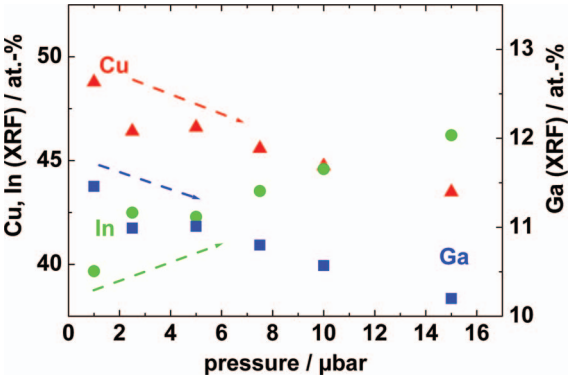

Fig. 3 Atomic concentration of precursors sputtered at pressures from 1 to 15 μbar, determined by XRF. An increasing copper and gallium content as well as a decreasing indium content for decreasing sputter gas pressure is observed.

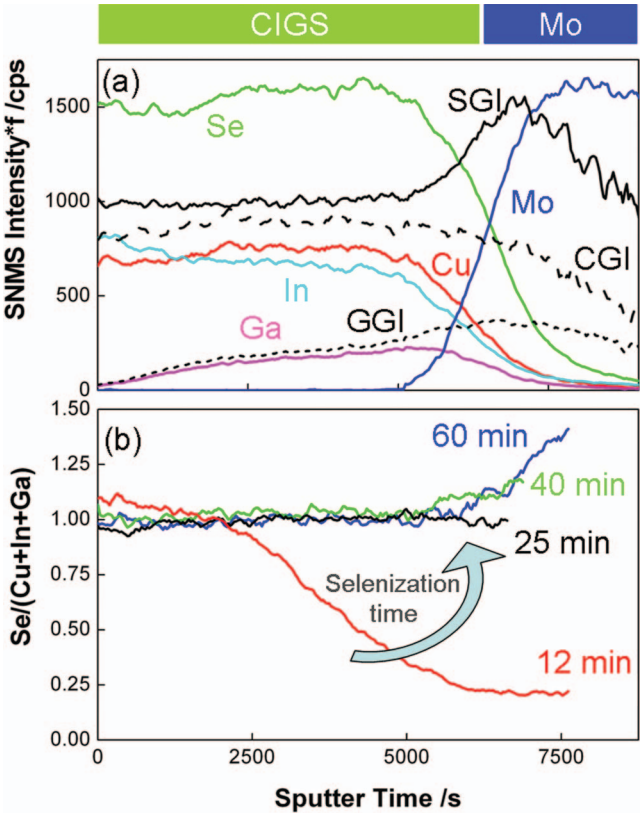

Fig. 4 SNMS depth profile of a selenized CIGS layer (a) on molybdenum-coated glass. The intensities were multiplied with sensitivity factors obtained by XRF. The ratios SGI = Se/(Cu+Ga+In), CGI = Cu/(Ga+In), and GGI = G/(Ga+In) are multiplied by a factor of 1000 for clarity. (b) shows the selenium portion that increases at the back contact with selenization time.

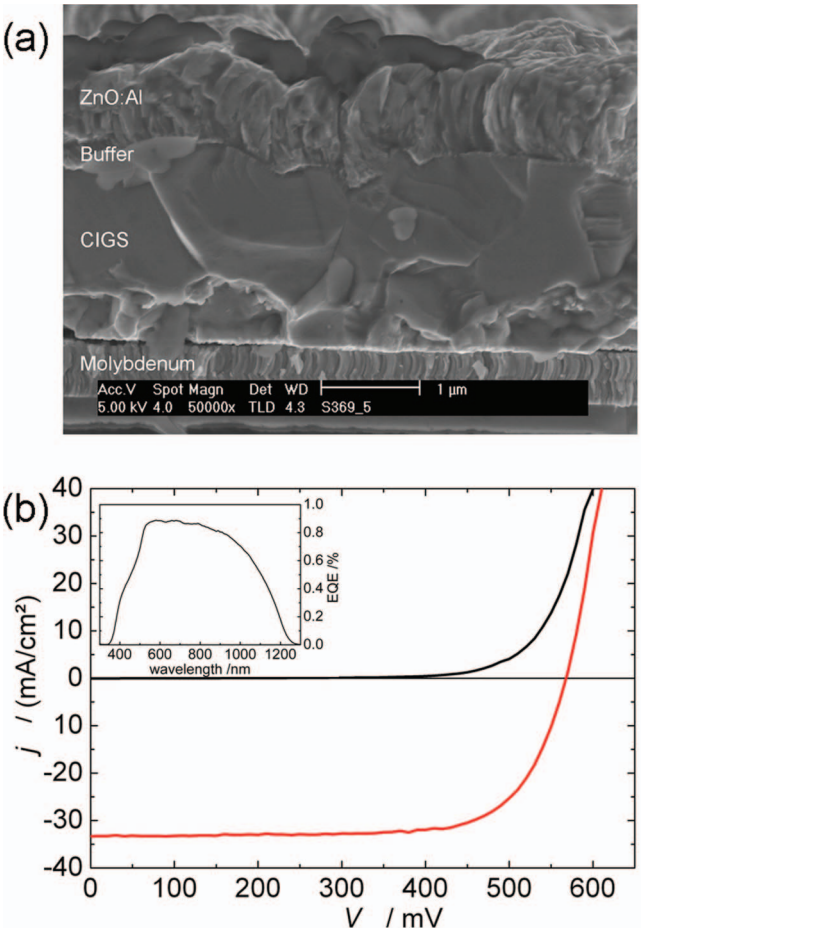

Fig. 5 (a) SEM image of a selenized layer completed to a solar cell. (b) Current-voltage characteristics and external quantum efficiency (inset) for the best cell. Eta = 13.7%; V_{oc} = 568 mV, FF = 72.4%; j_{sc} = 33.3 mA/cm^2, A = 0.24 cm^2.

at pressures from 1 to 15 μbar. We observe selective sputtering with a decreasing copper and gallium content as well as an increasing indium content for increasing sputter gas pressure. This phenomenon is probably related to differences in the sputter yield for elements with different atomic masses as is the case in an alloy target containing the light Cu and heavy In. It correlates with the decreasing thickness of the copper-rich underlayer with increasing pressure, as shown in the SEM cross-sections in Fig. 1.

3.2 Selenization and Solar Cells

XRD measurements of the CIGS layers are carried out for various selenization durations, as shown in Fig. 2. Already after 7 min selenization we find the CIGS phase beginning to evolve. For short selenization durations $Cu(In,Ga)_3Se_5$ and copper indium alloys can be seen.

Critical metallic phases are not detectable anymore in the diffraction pattern after 25 min of selenization, although shunting is still sometimes an issue. The shunting behavior could be related to incomplete CIGS transformation with residual (amorphous) metallic phases. Thus, although CIGS conversion is shown by XRD to be complete after about 25 min, a selenization time of 60 min is favorable in order to obtain maximum cell efficiencies.

Table 2 Current-voltage characteristics of different cells (A = 0.24 cm^2), without antireflective coating or metallic grids.

Sample	A	B	C	D	E	F	G
Eta (%)	12.2	12.7	12.4	12.1	13.7	13.2	12.3
Voc (mV)	489	527	516	520	568	527	524
FF (%)	69.5	71.6	68.4	69.7	72.4	73.7	70.1
jsc (mA/cm^2)	36.0	33.6	35.1	33.4	33.3	34.0	33.5

Alberts et.al investigated the influence of elemental Se or H_2Se, respectively, and found that Se-vapor-treated samples had nonuniform surface morphologies correlated with a relatively large variation in the Cu/In atomic ratio and Se concentration through the depth of the samples.[6] As shown in the SNMS depth profile [Fig. 4(a)] our samples are more homogeneous. We find a relatively constant CGI [Cu/(Ga+In) ratio] as well as a constant Se/(Cu+In+Ga) ratio throughout the depth of the sample. We only see an increase of Se content at the molybdenum back contact, which is heightened with selenization time [Fig. 4(b)]. We attribute this feature to the formation of molybdenum selenide. Furthermore, we observe a beneficial gallium gradient in the depth profile of the absorber layer.

A layer selenized for 60 min is shown in Fig. 5(a), indicating a polycrystalline structure. It has an atomic composition of Cu: 22.1 ± 0.5 at.%, In: 20.0 ± 0.9 at.%, Ga: 5.4±0.3 at.%, and Se: 52.6 ± 0.6 at.%, in agreement with the desired ratio for Cu(In,Ga)Se_2.

With these devices we can attain very good current-voltage characteristics and quantum efficiencies. Table 2 shows current-voltage characteristics of different cells that have been selenized in different runs and finished without antireflective coating or metallic grids. The accordant curves for the best cell with a conversion efficiency of 13.7% are shown in Fig. 5(b).

4 Conclusions

We investigated the film growth and selenization reaction of Cu-In-Ga precursor layers manufactured from a simple and cost-effective single-target sputter process and using a nonvacuum selenium vapor selenization reaction. The film growth during sputtering takes place via Cu- and In-rich segregated phase alloys. We could demonstrate highly efficient CIGS solar cells with cell efficiencies well above 13% with this approach.

References

1. P. Jackson, D. Hariskos, E. Lotter, S. Paetel, R. Würz, R. Menner, W. Wischmann, and M. Powalla, "New world record efficiency for Cu(In,Ga)Se_2 thin-film solar cells beyond 20%," *Prog. Photovoltaics* **19**, 894–897 (2011).
2. A. M. Gabor, J. R. Tuttle, D. S. Albin, M. A. Contreras, R. Noufi, and A. M. Hermann, "High-efficiency CuInxGa$_{1-x}$$Se_2$ solar cells made from (Inx,Ga$_{1-x}$)$_2$$Se_3$ precursor films," *Appl. Phys. Lett.* **65**(2), 198–200 (1994).
3. M. Marudachalam, H. Hichri, R. Klenk, R. W. Birkmire, W. N. Shafarman, and J. M. Schultz, "Preparation of homogeneous Cu(InGa)Se_2 films by selenization of metal precursors in H_2Se atmosphere," *Appl. Phys. Lett.* **67**, 3978–3980 (1995).
4. V. Probst, W. Stetter, W. Riedl, H. Vogt, M. Wendl, H. Calwer, S. Zweigart, K.-D. Ufert, B. Freienstein, H. Cerva, and F. H. Karg, "Rapid CIS-process for high efficiency PV-modules: development towards large area processing," *Thin Solid Films* **387**(1–2), 262–267 (2001).
5. V. Alberts, "Band gap optimization in Cu($In_{1-x}Ga_x$)($Se_{1-y}S_y$)$_2$ by controlled Ga and S incorporation during reaction of Cu-(In,Ga) intermetallics in H_2Se and H_2S," *Thin Solid Films* **517**(25), 2115–2120 (2009).

6. Y. Goushi, H. Hakuma, K. Tabuchi, S. Kijima, and K. Kushiya, "Fabrication of pentanary Cu(InGa)$(SeS)_2$ absorbers by selenization and sulfurization," *Sol. Energy Mater. Sol. Cells* **93**(8), 1318–1320 (2009).
7. S. Britting, A. Borkowski, C. Dütsch, R. Simon, and K.-U. van Ostern, "Development of novel target materials for Cu(In,Ga)Se-based solar cells," *Plasma Processes Polym.* **6**(1), S25–S28 (2009).
8. M. Schlott, A. Kastner, M. Schultheis, C. Simon, C. Stegmann, and M.-L. Goyallon, "Sputtering targets and thin film properties for thin film photovoltaic cells," in *24th European Photovoltaic Solar Energy Conference* (2009).
9. G. S. Chen, J. C. Yang, Y. C. Chan, L. C. Yang, and W. Huang, "Another route to fabricate single-phase chalcogenides by post-selenization of Cu–In–Ga precursors sputter deposited from a single ternary target," *Sol. Energy Mater. Sol. Cells* **93**(8), 1351–1355 (2009).
10. J.-C. Chang, C.-C. Chuang, J.-W. Guo, S.-C. Hsu, H.-R. Hsu, C.-S. Wu, and T.-P. Hsieh, "An investigation of $CuInGaSe_2$ thin film solar cells by using CuInGa precursor," *Nanosci. Nanotechnol. Lett.* **3**(2), 200–203 (2011).
11. M. Kaelin, D. Rudmann, F. Kurdesau, H. Zogg, T. Meyer, and A. N. Tiwari, "Low-cost CIGS solar cells by paste coating and selenization," *Thin Solid Films* **480–481**, 486–490 (2005).
12. S. Ahn, C. Kim, J. Yun, J. Lee, and K. Yoon, "Effects of heat treatments on the properties of Cu(In,Ga)Se_2 nanoparticles," *Sol. Energy Mater. Sol. Cells* **91**(19), 1836–1841 (2007).
13. M. Powalla and B. Dimmler, "Process development of high performance CIGS modules for mass production," *Thin Solid Films* **387**(12), 251–256 (2001).
14. M. Purwins, R. Enderle, M. Schmid, P. Berwian, G. Müller, F. Hergert, S. Jost, and R. Hock, "Phase relations in the ternary Cu–Ga–In system," *Thin Solid Films* **515**(15), 5895–5898 (2007).

Biographies and photographs of the authors not available.